Analysis of Sanding Parameters, Sanding Force, Normal Force, Power Consumption, and Surface Roughness in Sanding Wood-Based Panels

Bin Luo, Li Li,* Hongguang Liu, Meijun Xu, and Fangru Xing

The proper parameters of sanding with an abrasive sanding machine are significant to reduce energy consumption and to improve processing efficiency and quality. The influences of grit size (*G*), feed speed (*U*), sanding speed (*V*), and sanding thickness (T_s) on the sanding force (*sF*), normal force (*nF*), arithmetic mean deviation of profile (R_a), power consumption (*P*), and power efficiency (ε) were analyzed by the orthogonal method in this study. Fuzzy synthetic evaluation (*FSE*) was adopted to evaluate *sF*, *P*, and R_a comprehensively and to determine the optimum sanding parameters. For both medium density fiberboard (*MDF*) and particle board (*PB*), *G* has the greatest impact on R_a. For *MDF*, T_s and *G* have great impacts on *sF*, *G* is also the significant factor affecting *nF*, whereas the significant factors affecting *P* are *U* and *V*. For *PB*, *G*, *U*, and T_s have great impacts on *sF*, while *G* and T_s are the significant factors for *nF*. Significant factors for *P* are *V* and T_s. For *MDF* and *PB*, when the weight vector (*sF*, R_a) is (0.3, 0.7), the optimum schemes are $G_{80}U_{3m/min}V_{8.04,9.38,10.74m/s}T_{S0.2,0.3mm}$ and $G_{80}U_{3m/min}V_{9.38m/s}T_{S0.2mm}$, respectively, and when (*sF*, R_a) is (0.7, 0.3), the optimum schemes are $G_{80}U_{3,3.72m/min}V_{6.69,8.04,9.38m/s}T_{S0.2mm}$ and $G_{80}U_{3m/min}V_{8.04,9.38m/s}T_{S0.2mm}$, respectively. Additionally, when the weight vector (*P*, R_a) is (0.3, 0.7) or (0.7, 0.3), the optimum scheme is $G_{100}U_{2.52m/min}V_{5.35m/s}T_{S0.1mm}$.

Keywords: Medium density fiberboard; Normal force; Particleboard; Power efficiency; Sanding force; Sanding parameter; Surface roughness

Contact information: College of Materials Science and Technology, Beijing Forestry University, No.35 Tsinghua East Rd, Haidian District, Beijing.100083, P. R. China;
Corresponding author: bjfu_lili@126.com

INTRODUCTION

To improve surface lamination and painted quality, wood-based panels should be sanded prior to lamination and painted to eliminate the roughness of the material and the machining marks (Lin and Ho 2003; Vitosytė *et al.* 2012).

The sanding process consists of three processes: cutting, rubbing, and scribing. When the pressure on the work-piece is very small, grit only rubs the surface of the work-piece. With slightly increasing pressure, grit cuts and scribes the surface, but the proportion of scribing is higher than that of cutting. The normal cutting process cannot proceed until the pressure is sufficiently high. When grinding metal with a grinding wheel, the surface roughness *(R)* decreases with increasing scribing width (contact width minus cutting width) (Tan *et al.* 2012). A previous study indicated that *R* decreases with increasing sanding pressure when sanding 304 stainless steel with a sanding belt (Huang and Yang 2011).

Grit size (*G*) and feed speed (*U*) have great effects on the arithmetic mean deviation of profile (R_a) during the wood sanding process (Tan *et al.* 2012). Normally, with

increasing grit number, surface roughness decreases. In order to have a reliable assessment of the effect of processing (sanding), wood anatomical irregularities have to digitally be removed from the measured data, or they may disturb the results. This is valid for wood, but also for wood based panels. At the same time, other sanding parameters also affect the *R* of wood materials. In most cases, smoother surfaces can be obtained with greater pressure (Hendarto *et al.* 2006; Varasquim *et al.* 2012).

There are several factors that influence the sanding quality. One group of features is related to the wood material and machine, such as density, texture, moisture content, required precision, and stiffness of the sanding device (Shen 2005). The machining parameters, such as sanding speed (*V*), *U*, and *G*, are also important. It was found that the *U* and sanding thickness (T_s) influence the sanding force (*sF*) and normal force (*nF*) for sanding wood and medium-density fiberboard (*MDF*) (Liu and Li 2009). Simultaneously, the *nF* has significant impacts on the sanding quality and efficiency (Barcik and Samolej 2003; Siklienka and Ockajova 2003).

Power consumption (*P*) in the sanding process includes three parts: cutting power consumption, heating power consumption, and air resistance power consumption. Different sanding parameters cause different proportions of *P*. When sanding metal under a certain combination of sanding parameters, sanding efficiency was highest and degrees of grit wear and *P* were lowest, and therefore the greatest sanding quality was achieved (Coes 1971).

This study aims to determine the optimum sanding process using the orthogonal experimental method and fuzzy synthetic evaluation (*FSE*), and to analyze the relationships between *nF* and other parameters (*i.e.*, *sF*, *P*, power efficiency (ε), and R_a). The intention is to provide theoretical guidance for reducing energy loss and improving the efficiency and sanding surface quality.

EXPERIMENTAL

Materials

Experimental facilities

A sanding experimental machine equipped with a reciprocating motion worktable and calibrated sanding developed at Beijing Forestry University was used in this study. The calibrating roller is made of rubber, and the surface hardness is 25.0 HD. The work-piece and sensor were affixed to the worktable. The adjustable sanding thickness has an accuracy to 0.05 mm. The measuring equipment included a 3D force sensor (KISTLER 3257A; Switzerland), a charge-amplifier (KISTLER 5806; Switzerland), a signal analyzer (NEC Omniace II RA2300; Japan), a multi-function power meter (TUOKE TEPW994H8, China; accuracy ±5% FS ±2Ddigit, minimum sampling frequency 0.1s), and a surface roughness measuring instrument (Surtronic3+, UK; range is ±150 μm, accuracy is 10.0 nm, diamond stylus tip is in 90 ° cone shape, vertex is 5 μm in radius, and tracing speed is 1 mm/s).

Work pieces and sanding belts

MDF and particle board (*PB*) had a kiln -dried average density of 0.74 g/cm^3 and 0.99 g/cm^3, respectively, and surface hardness of 51.7 HD and 64.1 HD, respectively. The size of the work-pieces was 150 mm x 100 mm, with a thickness of 30 mm. One step of manufacturing process of *MDF* and *PB* is hot-pressing. During this process, the adhesive on the surface of panel solidifies very quickly (1 to 2 seconds) before the hot pressboard closes, which is caused by the heat emitted from the hot pressboard. So when the hot pressboard closes, the layer of solidified adhesive cannot combine with the fibers, and this layer is named of pre-cured layer (usually, the thickness is 3 to 4 mm). A pre-cured layer of work-piece was eliminated by sanding before the experiment. Additionally, 6 mm of two sides of the work-piece respectively can be used for testing, which is caused by the different densities of the *MDF* and *PB* through thickness direction. To make the tests accurate, for example, when the sanding parameters changed from $G_{a1}U_{b1}V_{c1}T_{sd1}$ to $G_{a2}U_{b2}Vc_2T_{sd2}$, the work-piece was sanded one time with $G_{a2}U_{b2}Vc_2T_{sd2}$ (data not collected), and available data were collected during the next three tests. The abrasive belts made by Tianjin Deerfos Co., Ltd. (China) consisted of twill base material, white fused alumina grit electro coated abrasive, and phenol formaldehyde resin adhesive.

Methods

Electric signals of *sF* and *nF*, which were generated by the force sensor during the sanding process, were captured by a signal collection device. The values of electric signals were transformed to the corresponding values of the forces. *P* and ε were acquired with a signal acquisition card. Each test was repeated three times to avoid any error. The *sF* measured in the test is the resultant force of the sanding tangential force (*sFt*) and radial force (*sFr*) in the horizontal direction, and the *nF* is the resultant force of *sFt* and *sFr* in the vertical direction. The testing system is shown in Fig. 1.

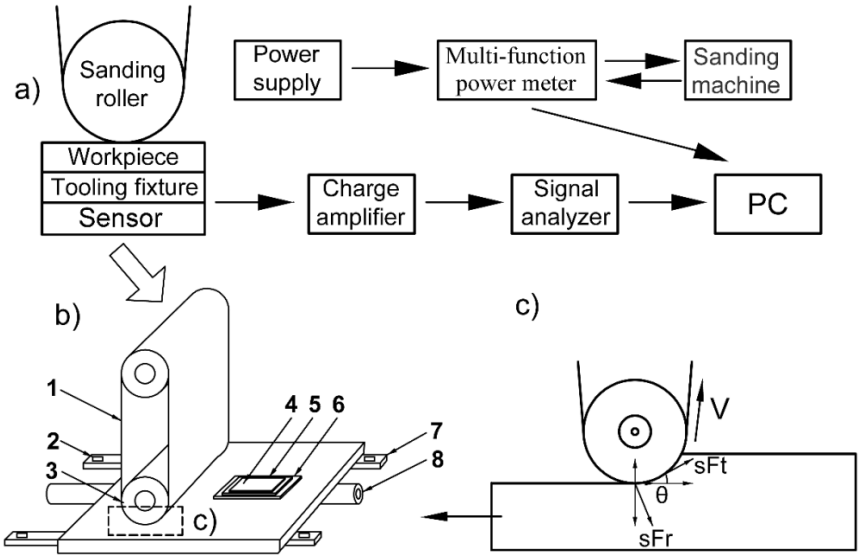

Fig. 1. Testing system: (a) Schematic of test system; (b) Schematic of testing machine; (c) Analysis of *sF* and *nF* (*sFt*-sanding tangential force; *sFr*-radial force; *θ*-angle between sanding speed and feed speed; *V*-sanding speed; (1) abrasive belt; (2) reciprocating control switch;(3) contacted roller; (4) work-piece; (5) tooling fixture; (6) KISTLER-3257A sensor; (7) rail; (8) ball screw actuating device)

The major factors considered in this study were as follows: grit size (*G*), feed speed (*U*), sanding speed (*V*), and sanding thickness (T_s). Each factor had five levels (as shown in Table 1), resulting in a [L25 (5^6)] orthogonal table (as shown in Table 2). The values of *U* were low because the workbench moved through a rail system instead of by conveyer belt. Additionally, in order to prevent error caused by vibrations, the *V* also cannot be very fast.

Table 1. Orthogonal Factors and Levels

Levels	Granularity (grit)	Feed speed (m/min)	Sanding speed (m/s)	Sanding thickness (mm)
1	40	2.52	5.35	0.1
2	60	3.00	6.69	0.2
3	80	3.72	8.04	0.3
4	100	4.44	9.38	0.4
5	120	5.16	10.74	0.5

Table 2. Orthogonal Table

Numbers	Grit size (*G*)	Feeding speed (*U*)	Sanding speed (*V*)	Sanding thickness (T_s)
1	1	1	1	1
2	1	2	2	2
3	1	3	3	3
4	1	4	4	4
5	1	5	5	5
6	2	1	2	3
7	2	2	3	4
8	2	3	4	5
9	2	4	5	1
10	2	5	1	2
11	3	1	3	5
12	3	2	4	1
13	3	3	5	2
14	3	4	1	3
15	3	5	2	4
16	4	1	4	2
17	4	2	5	3
18	4	3	1	4
19	4	4	2	5
20	4	5	3	1
21	5	1	5	4
22	5	2	1	5
23	5	3	2	1
24	5	4	3	2
25	5	5	4	3

In the actual production, improving quality of products and reducing energy consumption are both important; *sF* and *P* reflect the energy consumption, and R_a reflects the sanding quality, so *sF*, *P*, and *R* should be comprehensively evaluated for the optimal sanding process. Fuzzy synthetic evaluation (*FSE*) was adopted to comprehensively

evaluate these three factors and determine the optimal sanding parameters. *FSE* applies a comprehensive evaluation based on fuzzy mathematics. It changed the qualitative evaluation into quantitative evaluation according to the fuzzy membership degree theory. And to make a comprehensive evaluation of multiple indices affected by various influence factors (Shen and Wen 2005). The key of comprehensive evaluation is to determine the weight vectors of evaluation indices. In this study, the method used to determine the weight vectors was the expert evaluation method. Expert evaluation, which is similar to peer review, is a method that the evaluation system and the weight vector of evaluation index is determined by intuitive assessment of the experts under their knowledge and experience. The evaluation results of this paper are the average results of eight experts in the field of wood-based panels (Zhou and Wei 2006). Considering the actual processing needs, the weight vectors of the three comprehensive evaluation indices are as follows: (sF, R_a) are(0.3, 0.7); (sF, R_a) are (0.7, 0.3); (P, R_a) are (0.3, 0.7);and (P, R_a) are (0.7, 0.3), when (sF/P, R_a)= (0.7, 0.3) means that power consumption is the primary review indicator, and when (sF/P, R_a)= (0.3, 0.7), it means that the product quality is the main indicator.

RESULTS AND DISCUSSION

Orthogonal Analysis

Table 3 and Fig. 2 show the results of the orthogonal analysis of sF, nF, P, ε, and R_a.

Table 3. Variance Analysis Table

Factors	sF		nF		P		ε		R_a	
	Mean square	F	Mean square	F	Mean square	F	Mean square	F	Mean square	F
					MDF					
G	361	**5.2**	1089	**5.2**	5368	1.4	0.00016	1.4	79.1	**113.2**
U	127	1.8	327	1.6	26284	**6.8**	0.00008	0.7	0.9	1.3
V	77	1.1	256	1.2	150298	**38.9**	0.00016	1.4	0.8	1.1
T_s	389	**5.6**	713	3.4	6472	1.7	0.00018	1.5	0.3	0.5
Error	69		209		3864		0.00012		0.7	
	Orders of priorities of factors' influence									
	$T_s>G>U>V$		$G>T_s>U>V$		$V>U>T_s>G$		$T_s>G=V>U$		$G>V>U>T_s$	
					PB					
G	190	**15.2**	849	**10.6**	6884	0.4	0.00008	0.4	124.3	**23.7**
U	127	**10.1**	272	3.4	6162	0.4	0.00030	1.4	1.1	0.2
V	26	2.1	117	1.5	167811	**10.7**	0.00056	2.6	5.3	1.0
T_s	537	**42.8**	921	**11.5**	82613	**5.3**	0.00026	1.2	9.0	1.7
Error	13		131		15652		0.00022		5.2	
	Orders of priorities of factors' influence									
	$T_s>G>U>V$		$T_s>G>U>V$		$V>T_s>G=U$		$V>U>T_s>G$		$G>T_s>V>U$	

Boldtype: overpass $F_{0.05}= 3.8$, boldtype with underline: overpass $F_{0.01}= 7.0$

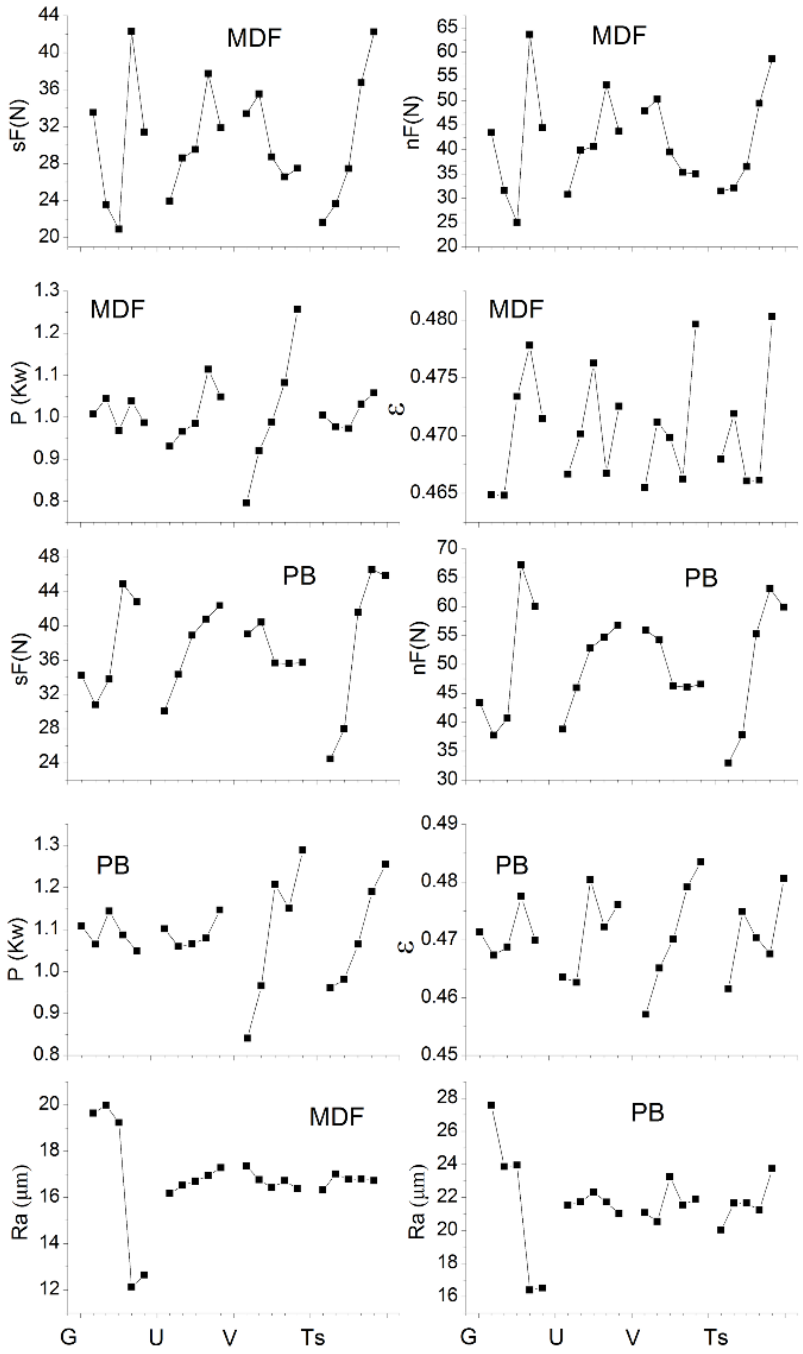

Fig. 2. Orthogonal analysis chart

In order to distinguish the impact factors more precisely, the inspection levels adopted in this study were α=0.05 and α= 0.01, respectively. The values on vertical of axes (Fig. 2) are the average values of *sF*, *nF*, *P*, and ε. For example, when *G*=40, there are five experimental results of *nF* in the orthogonal experiment (Table 2), and the value of *nF* (*G*=40) is an average value of these five results.

For *MDF*, *G* and T_s had prominent impacts on *sF*, but the degree of distinction between these two factors was low; moreover, *G* also influenced *nF* significantly. *sF* and *nF* increased with increasing T_s (Fig. 2). *V* had the greatest impact on *P*, and *U* had a lower

effect. For *PB*, T_s, *G*, and *U* were the very significant influence factors of *sF*, and T_s was the most significant one. T_s also had the greatest impact on *nF*, and the impact of *G* was a little smaller than that of T_s. Compared to *MDF*, *V* was also the most influential factor for *P*; however, the second most influential factor was T_s. Among all the sanding parameters, *G* had the greatest impact on R_a, but no factor had a prominent impact on ε for both materials. The density and surface hardness of *PB* were greater than those of *MDF*, so *sF* and *nF* were greater for *PB* than they were for *MDF*.

During the sanding process, cutting with grit generates cutting power consumption (*Pc*), and *Pc* depends on *sF* and *V* when θ is negligible, as shown in Eq. (1), Eq. (2), and Eq. (3). In the actual production process, θ is very small. Within limits, increasing *V* causes decreasing *sF* and *P* (the number of cutting edges increases). However, sanding air resistance increases because of the severe turbulence generated by a high-speed rotational abrasive belt (high-speed *V*).

$$Pc = sF_t(V + U/\cos\theta) \tag{1}$$

$$\lim_{Ts\to 0} sF_t = \lim_{\theta\to 0} sF/\cos\theta = sF \tag{2}$$

$$\lim_{Ts\to 0} sF_t(V + U/\cos\theta) = sFV \tag{3}$$

Nevertheless, the *P* is not only caused by cutting, but also by friction and air resistance (heat loss). Different sanding parameters influence not only *sF* and *V*, but also other forces. This is the reason for the different change laws between *P* and *sF*.

During the sanding process, the abrasive grit in the abrasive belt was equivalent to the cutting edges, and there were spaces among grit which provided a "chip flute" for the abrasive belt in normal cutting and discharged the sanding dust. These spaces were reduced when the density of the grit increased in per unit area or sanding dust filled the spaces; under these conditions, the sanding heat and resistance increased and sanding efficiency decreased.

Within limits, when other sanding parameters were invariant, cutting edges involved in the cutting process in per unit time increased with increasing *V*. Thus, removal of one cutting edge decreased when the total sanding removal was constant in unit time, which led to decreasing forces. However, when *V* surpassed a critical value, the sanding dust and glue of the work-piece rapidly filled the space between the grit and blocked the grit, and the grit became blunt and the "chip flute" narrowed (*i.e.*, blunting and blocking phenomenon). There was not enough time for the abrasive belt to fully discharge the dust. This phenomenon became more and more apparent with increasing *V*. The size of the chips (the structural unit of *PB*) is much larger than that of wood fibers (the structural unit of *MDF*). It was difficult for chips to fill the spaces within the sanding grit, so there was not a serious blunting and blocking phenomenon during sanding of *PB*.

A wood-based panel can buffer the impulse force to a limited extent during the feed process. However, the materials will deform when the impulse force surpasses the elastic limit. When other sanding parameters were constant, with increasing *U*, the total quantity of sanding removal in per unit time increased; thus removal of one cutting edge grew, which caused increasing *sF* and *nF*. Abrasive grit became finer with increasing *G*; therefore, under the same conditions of *U*, *V*, and T_s, the quantity of grit in per unit area increased with increasing *G*, then the quantity of cutting edges in per unit time increased in sanding process. However, the forces did not decrease with the increasing *G* all the time,

which can be explained by the narrowed space among the grit (Fig. 2). The general trend is that R_a decreases with increasing G, which can be seen from Fig. 3. Surface roughness should decrease with increasing grit number if the other sanding parameters are kept constant and the influence of wood anatomical irregularities is removed (the sanding gaps are smaller when the grit number becomes greater, but, at the same time, the amount of wood detached from the surface decreases). However, R_a does not keep decreasing with increasing G due to the gaps between structural units (*i.e.*, *MDF* and *PB*), the fiber direction (*i.e.*, *MDF*), and the textures of chips (*i.e.*, *PB*). Because chips, the structural units of *PB*, inherit wood characteristics such as wood texture and knots, the arrangement of chips is irregular, and this results in some unpredictable experimental results.

Relevancy Analysis among *nF*, ε, *P*, R_a, and *sF*

Pressure (*nF*) is easily measured in the sanding process, thus, the analysis of relationships between *nF* and other factors is more practical (the values were the results of an orthogonal experiment). Figure 3 indicates that there is a linear relationship between *nF* and *sF*, and this result can also be proven by a physical model ($nF=sF\ tan\theta$).

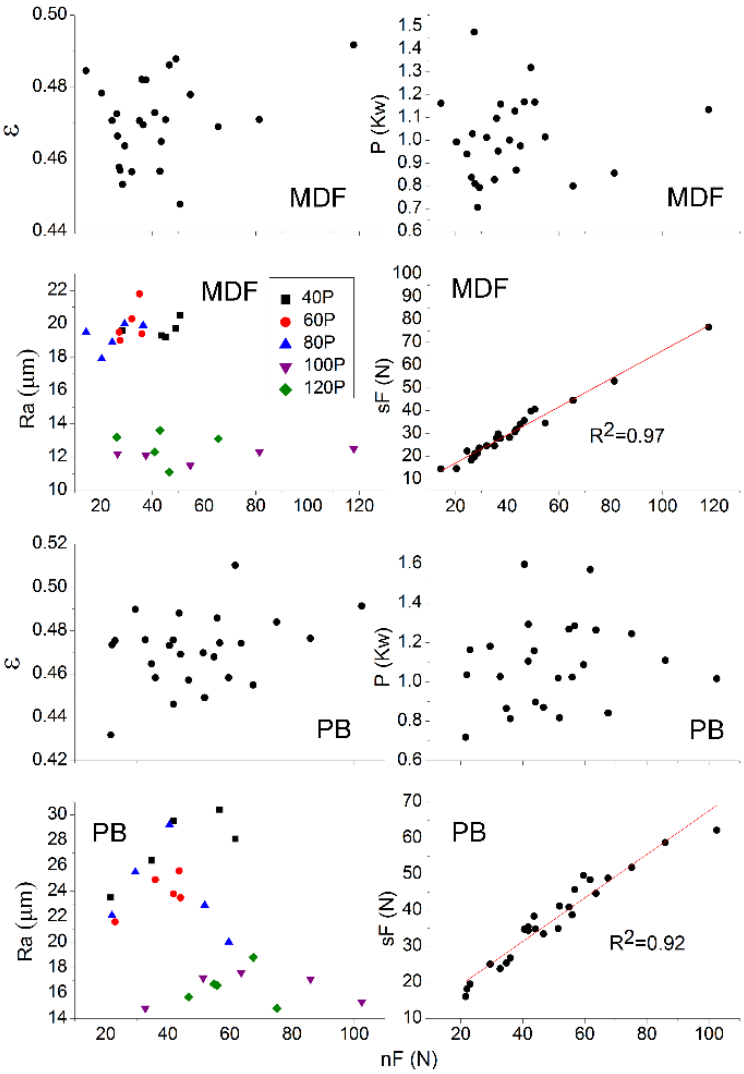

Fig. 3. Relevancy analysis among *nF* and other indices

In consideration of the great impact of G on R_a, the relationships between nF and different values of G are compared. Different from previous studies (Varasquim *et al*. 2012), no relationship between nF and R_a can be found, and the relationships of nF with P and ε are also not obvious. The surface becomes smoother (scribing width increase) with increasing pressure when sanding metal (Tan *et al*. 2012); however, for wood-based panels, the textural and inhomogeneous characteristics cannot be neglected.

Optimum Schemes

The optimum schemes for different indices are listed in Table 4. As can be deduced from Fig. 2, for sF, nF, P, and R_a, the minimum values are the optimal sanding parameters, but for ε, the maximal values are appropriate (low power loss).

Table 4. Optimum Scheme for Single Index

Optimum index	Optimum scheme	
	MDF	*PB*
sF	$G_3U_1V_4T_{s1}$	$G_2U_1V_4T_{s1}$
nF	$G_3U_1V_5T_{s1}$	$G_2U_1V_4T_{s1}$
P	$G_3U_1V_1T_{s3}$	$G_5U_2V_1T_{s1}$
ε	$G_4U_3V_5T_{s5}$	$G_4U_3V_5T_{s5}$
R_a	$G_4U_1V_5T_{s1}$	$G_4U_5V_2T_{s1}$

The optimal sanding parameters, which were analyzed with the *FSE* method, are shown in Table 5.

Table 5. Comprehensive Optimum Scheme of Sanding Parameters

Weight vector		(sF, R_a)=(0.3, 0.7)	(sF, R_a)=(0.7, 0.3)
Optimum scheme	*MDF*	$G_3U_2V_{345}T_{s23}$	$G_3U_2V_4T_{s2}$
	PB	$G_3U_{23}V_{234}T_{s2}$	$G_3U_2V_{34}T_{s2}$
Weight vector		(P, R_a)=(0.3, 0.7)	(P, R_a)=(0.7, 0.3)
Optimum scheme	*MDF*	$G_4U_1V_1T_{s1}$	$G_4U_1V_1T_{s1}$
	PB	$G_4U_1V_1T_{s1}$	$G_4U_1V_1T_{s1}$

CONCLUSIONS

1. The results of Table 4 take only a single factor into consideration. This method (orthogonal experiment) is suitable for a single optimization goal. When sanding wood-based panels, G has a large impact on sF, nF, and R_a, and V is a significant influencing factor on P; however, sanding parameters do not have a prominent impact on ε. A linear relationship exists between sF and nF, but there is no obvious relationship between pressure (nF) and R_a.
2. Taking a comprehensive consideration of sanding efficiency and sanding quality, the optimum schemes of sanding parameters are as follows. For *MDF* and *PB*, when the weight vector (sF, R_a) is (0.3, 0.7), the optimum schemes are $G_{80}U_{3m/min}V_{8.04,\ 9.38,\ 10.74m/s}T_{s0.2,\ 0.3mm}$, and $G_{80}U_{3m/min}V_{9.38m/s}T_{s0.2mm}$, respectively, and when (sF, R_a) is (0.7, 0.3), the optimum schemes are $G_{80}U_{3,3.72m/min}V_{6.69,8.04,9.38m/s}T_{s0.2mm}$, and $G_{80}U_{3m/min}V_{8.04,9.38m/s}T_{s0.2mm}$, respectively. Additionally, when the weight vector (P, R_a) is (0.3, 0.7) or (0.7, 0.3), the optimum scheme is $G_{100}U_{2.52m/min}V_{5.35m/s}T_{s0.1mm}$.

ACKNOWLEDGMENTS

This paper was financially supported by the Special Fund for Forestry Research in the Public Interest (Project 201204703-B2) and the Fundamental Research Funds for the Central Universities (BLYX200903).

REFERENCES CITED

Barcik, S., and Samolej, A. (2003). "Experimental investigation of sanding process on disc sander," *Wood Res.* 48, 36-42.

Coes, L. (1971). *Abrasives*, Springer-Verlag, New York.

Hendarto, B., Shayan, E., Ozarska, B., and Carr, R. (2006). "Analysis of roughness of a sanded wood surface," *International Journal of Advanced Manufacturing Technology* 28(7-8), 775-780. DOI: 10.1007/s00170-004-2414-y

Huang, Y., and Yang, C.Q. (2011). "Experimental research on abrasive belt grinding for 304 stainless steel," *China Mechanical Engineering* 22(3), 291-295.

Lin, Z. C., and Ho, C. Y. (2003). "Analysis and application of grey relation and ANOVA in chemical-mechanical polishing process parameters," *International Journal of Advanced Manufacturing Technology* 21(1), 10-14. DOI: 10.1007/s001700300001

Liu, B., and Li, L. (2009). "Sanding force of wood and medium-density fiberboard," *Journal of Beijing Forestry University* 31, 197-201.

Shen, B. X., and Wen, C. J. (2005). *Experimental Design and Engineering Application*, Chinese Metrology Press, Beijing.

Shen, F. (2005). "Sanding technique (2)," *China For. Prod. Ind.* 32, 44-45.

Siklienka, M., and Ockajova, A. (2003). "Analysis of cutting forces during sanding of native wood," *Wood Res.* 48, 15-21.

Tan, P. L., Sharif, S., and Sudin, I. (2012). "Roughness models for sanded wood surfaces," *Wood Sci. Technol*. 46(1-3), 129-142. DOI: 10.1007/s00226-010-0382-y

Vitosytė, J., Ukvalbergienė, K., and Keturakis, G. (2012). "The effects of surface roughness on adhesion strength of coated ash (*Fraxinus excelsior* L.) and birch (*Betula* L.) wood," *Materials Science* 18(4), 347-351. DOI: 10.5755/j01.ms.18.4.3094

Varasquim, F. M. F. D. A., Alves, M. C. D. S., Gonçalves, M. T. T., Santiago, L. F. F., and de Souza, A. J. D. (2012). "Influence of belt speed, grit sizes and pressure on the sanding of *Eucalyptus grandis* wood," *Cerne* 18(2), 231-237. DOI: 10.1590/S0104-77602012000200007

Zhou, Y. F., and Wei, F. J. (2006). "Determination of expert's weight in comprehensive evaluation," *Industrial Engineering Journal* 9(5), 23-27.

Article submitted: July 15, 2014; Peer review completed: September 14, 2014; Revised version received and accepted: October 2, 2014; Published: October 27, 2014.